# SOIL DYNAMICS AND LIQUEFACTION

A.S. CAKMAK

# SOIL DYNAMICS AND LIQUEFACTION

Edited by

A.S. CAKMAK

Department of Civil Engineering, Princeton University, Princeton, N.J. 08544, U.S.A.

ELSEVIER Amsterdam – Oxford – New York – Tokyo 1987

Co-published with

COMPUTATIONAL MECHANICS PUBLICATIONS Southampton — Boston — Los Angeles 1987 ELSEVIER SCIENCE PUBLISHERS B.V. Sara Burgerhartstraat 25, P.O. Box 211 1000 AE Amsterdam, The Netherlands

Distributors for the United States and Canada:

ELSEVIER SCIENCE PUBLISHING COMPANY INC. 52 Vanderbilt Avenue New York, N.Y. 10017

COMPUTATIONAL MECHANICS PUBLICATIONS Ashurst Lodge, Ashurst Southampton, SO4 2AA, U.K.

## British Library Cataloguing in Publication Data

Soil dynamics and liquefaction.
1. Soil dynamics
1. Cakmak, A.S.
624.1'5136 TA710

ISBN 0-905451-69-4

Library of Congress Catalog Card number 87-70778

ISBN 0-444-98958-7 (Vol.42) Elsevier Science Publishers B.V. ISBN 0-444-41662-5 (Series) ISBN 0-905451-69-4 Computational Mechanics Publications, UK ISBN 0-931215-57-9 Computational Mechanics Publications, USA

This Work is subject to copyright. All rights are reserved, whether the whole or part of the material is concerned, specifically those of translation, reprinting, re-use of illustrations, broadcasting, reproduction by photocopying machine or similar means, and storage in data banks.

© Computational Mechanics Publications Elsevier Science Publishers B.V. 1987

Printed in Great Britain by Adlard and Son Limited, Dorking

The use of registered names, trademarks etc. in this publication does not imply, even in the absence of a specific statement, that such names are exempt from the relevant protective laws and regulations and therefore free for general use.

### **PREFACE**

The Earthquake Engineering Community has a long way to go, as despite advances in the field of Geotechnical Earthquake Engineering, year after year earthquakes continue to cause loss of life and property and leave continued

human suffering in their wake in one part of the world or another.

We hope to provide the Earthquake Engineering Community with a forum to help develop further techniques and methods through the exchange of scientific ideas and innovative approaches in Soil Dynamics and Earthquake Engineering, by means of this volume and its companion volumes. This volume covers the following topics: Constitutive Relations in Soil Dynamics, \* Liquefaction of Soils and Experimental Soil Dynamics and contains edited papers selected from those presented at the 3rd International Conference on Soil Dynamics and Earthquake Engineering, held at Princeton University, Princeton, New Jersey, USA, June 22-24, 1987.

The editor wishes to express sincere thanks to the authors who have shared their expertise to enhance the role of mechanics and other disciplines as they

relate to earthquake engineering.

The editor also wishes to acknowledge the aid and support of Computational Mechanics Publications, Southampton, England, the National Center for Earthquake Engineering Research, SUNY, Buffalo, NY, and Princeton University, in making this conference a reality.

A.S. Cakmak June 1987

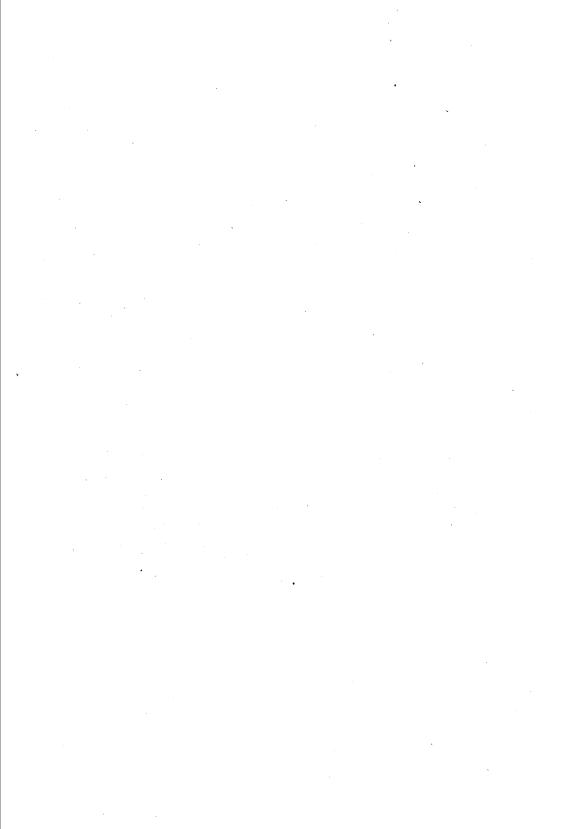
## CONTENTS

## **SECTION 1: CONSTITUTIVE RELATIONS IN SOIL DYNAMICS**

Computational Approach to Soil Dynamics O. C. Zienkiewicz, A. H. C. Chan, M. Pastor and T. Shiomi	3
The Development of Constitutive Relationship for Seismic Pore Pressure S.K. Bhatia, S. Nanthikesan	19
Effect of Frequency Content on Dynamic Properties of Cohesive Soils M.S. Aggour, K.S. Tawfiq and F. Amini	31
The Markov Framework for Modeling Uncertainties in Soil Constitutive Behavior H. Benaroya, G. Goldstein	41
An Anisotropic Hardening Model for Sand Subjected to Cyclic Loading H. Hirai	53
SECTION 2: LIQUEFACTION OF SOILS	
Analysis of Porewater Pressures in Seismic Centrifuge Tests W.D. Liam Finn, M. Yogendrakumar, N. Yoshida and H. Yoshida	71
Earthquake Induced Forces on Retaining Walls R.M. Bakeer, S.K. Bhatia	87
Risk Analysis of BRPL Compressor (Offsites) Foundations N. Puri, K. Kumar and S. Prakash	97
Cyclic Hardening of Sand During Earthquake Events U. Guettler, G. Thiel and H.L. Jessberger	107
Estimation of Bridge Foundation Stiffness from Forced Vibration Data C. B. Crouse, B. Hushmand	123
A Parametric Study of Effect of Vibration on Granular Soils P. W. Chang, Y.S. Chae	137
EQGEN86 – An Artificial Earthquake Simulation Program N. Y. Chang, B. H. Lien and M. J. Huang	153
On the Behavior of Soils During Earthquakes - Liquefaction G. Castro	169
Liquefaction of Shock Loaded Saturated Sand G.E. Veyera, W.A. Charlie	205

. Seismic Response of Pore Water Pressure in Surface Sand Layer E. Yanagisawa, H. Ohmiya and T. Shimizu	221
A Study of Earthquake Resistance of Highway Abutments During Liquefaction T. Ishibashi, M. Noda, K. Tanaka, H. Ikemi, M. Kamata and M. Nakam	231 uura
Assessing the Effects of Potential Liquefaction + A Practising Engineer's Perspective E.E. Rinne	
SECTION 3: EXPERIMENTAL SOIL DYNAMICS	*
Volume Change Behavior of Granular Soil Columns During Vibration G.M. Norman-Gregory, E. T. Selig	255
Cyclic Behavior of a Clay: Experiment and Modelling W. Y. Sheu, N. Y. Chang	269
Cyclic Triaxial Tests at Low Stresses for Parameter Determination A. Bezuijen, A. G. I. Hjortnaes-Pedersen and F. Molenkamp	283
Laboratory Prototype of In Situ Cyclic and Dynamic Geotechnical Testing System R. Henke, W. Henke	299
High Resolution Measurement of Shear Modulus of Clay Using Triaxial Vane Device S. Pamukcu, J. N. Suhayda	307
Model Tests for Earthquake Simulation of Geotechnical Problems R. V. Whitman, H. Klapperich	<b>32</b> 3
Experiments and Analysis for the Hysteresis Characteristics of Soil A. Hara, Y. Kiyota, Y. Sakai, H. Takano and T. Aoyagi	337
Shear Moduli and Damping Characteristics of Kosovo High Plasticity Clays N. Dzeletović, T. Paskalov	343
Numerical Modelling of Membrane Penetration Effects on Undrained Triaxial Tests J. R. Raines, R. I. Borja, H. Anwar and R.B. Seed	353
Cyclic Properties of Soils Within a Large Range of Strain  Amplitude  P. Y. Hicher, M.S. El Hosri and M. Homsi	<b>3</b> 65

## SECTION 1: CONSTITUTIVE RELATIONS IN SOIL DYNAMICS



## Computational Approach to Soil Dynamics

O.C. Zienkiewicz, A.H.C. Chan

Institute for Numerical Methods in Engineering, University College of Swansea, Swansea SA2 8PP, U.K.

M. Pastor

Centro de Estudios y Experimentacion de Puertos y Costas, Madrid, Spain T. Shiomi

DIANA co-ordinator, Takenaka Komuten Construction Company, Tokyo, Japan

#### INTRODUCTION

Engineering problems of Soil Dynamics can be formulated satisfactorily by taking into account full interaction of the fluid and soil phases of the material. The governing the interaction of the solid and fluid media were first established for quasi-static phenomena in 1941 by Biot extended them to dynamics. Later, owing to increasing interest in non-linear applications, a generalized incremental form was devised by Zienkiewicz et al., Prevost and others, in which large strain and non-linear behaviour are included. Various possible numerical solution methods to the generalized Biot formulation has been presented by Zienkiewicz Suiomii. In this paper, we will present the u-p formulation2 which retains the displacement of the soil skeleton and the pore fluid pressure as the primary unknowns.

Undrained behaviour seldom occurs even in very rapid carthquake phenomena and for this reason the full set of coupled equations of motion needs to be solved. The Research group at the Institute for Numerical Methods in Engineering at Swansea and the Diana Project in Japan have established now a series of programs capable of dealing fully with such phenomena.

The key to the satisfactory solution of the problem is of course in the correct constitutive relation. Although no ideal relation has yet been established very effective models capable of reproducing adequately static and dynamic behaviour of sands have been devised by the authors. These models respond satisfactorily to most of the standard triaxial tests and require a small number of parameters. The outline of the model structure will be presented in this paper but of course

the main test is its satisfactory performance in a true engineering situation.

It is very difficult in earthquake problems to find satisfactory test problems and for this reason we have concentrated on specially commissioned tests on the Cambridge Centrifuges's in which real models of structures and their foundations are used and full data on input of earthquake, pressure generation and deformations are available. It will be shown that excellent predictions can be made in all such cases and clearly therefore the techniques presented are applicable to the solution of real problems.

#### THE U-P FORMULATION AND TIME DOMAIN SOLUTION

In this section, we will study the behaviour of the solid 'skeleton' of soil and the fluid flow seperately. Later we will present the SSpj time stepping scheme for the time domain solution. Thus, for the solid phase, we have to solve the equilibrium equation

$$\sigma_{ij,j} + \rho g_i = \rho u_i$$
 (1)

with

$$d\sigma_{ij}'' = d\sigma_{ij} + \alpha \delta_{ij} dp \qquad (2)$$

$$d\sigma_{ij}^{\parallel} = D_{ijkl} \left( ds_{kl} + ds_{ki}^{\circ} \right)$$
 (3)

where

$$\alpha = 1 - K_{T} / K_{S} \tag{4}$$

For small strain and deformation

$$de_{ij} = (du_{i,j} + du_{j,i})/2$$
 (5)

The equilibrium equation has to be solved in conjunction with appropriate boundary conditions for displacement  $u_i$ , total stress  $\sigma_{ij}$ , and pore fluid pressure p. The equation (2) is the modified effective stress equation. In order to account for the compressibility of the soil particles, coefficient  $\alpha$  is introduced which depends on  $K_T$  is the bulk modulus of the soil skeleton and  $K_S$  that of the soil grains. The equation (3) relates the change in the modified effective stresses to the strain increment by the appropriate constitutive equations in which  $D_{ijkl}$  defines a tangential constitutive matrix and  $v_{ij}$  the 'initial' strain. However, the tensor  $v_{ij}$  depends upon the effective stress with  $v_{ij}$  equal to unity in equation (2) rather than the modified effective stress, this is the well-known effective stress concept in soil mechanics.

Under dynamic or slow transient conditions, the fluid acceleration relative to the soil skeleton can be neglected. Hence we can write an extended (D'Arcy) flow equation

$$-(k p_{i})_{i} + \alpha \epsilon_{i} -(k \rho_{f} g_{i})_{i} + (k \rho_{f} \ddot{u}_{i})_{i} + \dot{p}/Q = 0$$
 (6)

In the above equation k is the permeability coefficient, garavity component. Once again the appropriate boundary condition on the pressure need to be imposed. Here Q is a parameter defining the compressibility of the fluid, solid grains etc., and this is given approximately as

$$1/Q = n/K_f + (a - n)/K_S$$
 (7)

In equation (7) n is the porosity and Kf is the bulk modulus of the fluid. Frequently it is assumed that 1/Q is zero but generally this compressibility is non-negligible. The acceleration term in equation (7) has negligible influence and its retention is computationally undesirable, so it is left out in the further derivation.

With usual spatial Finite Element discretization assumed for  ${\bf u}$  and  ${\bf p}$  as

$$\underline{\mathbf{u}} = \underline{\underline{N}}_{\underline{\mathbf{u}}} \quad \underline{\underline{\mathbf{v}}} \quad \text{and} \quad \underline{\underline{\mathbf{p}}} = \underline{\underline{\underline{N}}}_{\underline{\underline{\mathbf{p}}}} \quad (8)$$

The application of Galerkin procedures? results in the following discrete equation with which the appropriate boundary conditions are incorporated in the forcing terms.

$$\underline{\underline{M}} \stackrel{=}{\underline{u}} + \int_{\Omega} \underline{\underline{B}}^{T} \underline{\underline{\sigma}}^{"} d\Omega - \underline{\underline{Q}} \underline{\underline{p}} = \underline{\underline{f}}_{1}$$
 (9a)

$$\underline{\underline{H}} \, \underline{\underline{p}} + \underline{\underline{Q}}^{T} \, \underline{\underline{u}} + \underline{\underline{S}} \, \underline{\underline{p}} = \underline{\underline{f}}_{2}$$
 (9b)

where the matrix  $\underline{M}$  is the mass matrix,  $\underline{B}$  the strain matrix.  $\underline{\underline{H}}$  the permeability matrix,  $\underline{\underline{Q}}$  connecting matrix and  $\underline{\underline{S}}$  the compressibility matrix, for exact definition of these matrices see reference 2.

#### TIME DOMAIN SOLUTION

The semi-discrete equation system (9) presents even in its linear form a nonsymmetric structure which leads to many computational difficulties if it is simply treated as a single set of equations. It is, however, quite simple to arrive at symmetric equation systems if the temporal discretization is applied individually to each of the equations. We show here the essential steps of this discretization using the SSpj algorithm of time stepping<sup>9-11</sup> in its lowest applicable order. This algorithm is derived on the basis of a Galerkin process in time with the assumption of an assumed expansion of the variables.

We write thus for a single time step  $t_n$  to  $t_{n+1} = t_n + \Delta t$ 

$$\frac{\ddot{\underline{u}} = \ddot{\underline{u}}_n + \dot{\underline{u}}_n \tau + \underline{a} \tau^2 / 2 \tag{10a}$$

$$\underline{\mathbf{p}} = \underline{\mathbf{p}}_{\mathbf{p}} + \underline{\mathbf{g}} \mathbf{\tau} \tag{10b}$$

where 
$$0 \le \tau = t - t_n \le \Lambda t$$
 (11)

and the initial values of  $\bar{u}_n$ ,  $\dot{\bar{u}}_n$  and  $\bar{p}_n$  are known.

Trial functions in equation (10) are now inserted into equations (9) and by weighting each of these with functions W and W respectively and integrating from  $\gamma=0$  to  $\gamma=\Delta t$  we shall obtain an algebraic equation system from which the unknown vectors  $\underline{\alpha}$  and  $\underline{\beta}$  can be found.

At this stage a further assumption concerning non-linear terms of equation (9) must be made. We shall assume in particular that the term giving the internal force varies linearly with  $\underline{u}$  in the interval  $\Delta t$ , i.e. that we can write

$$\int_{\Omega} \underline{B}^{T} \underline{\sigma}^{i_{l}} d\Omega = \underline{P}(\underline{\overline{u}}) = \underline{K}\underline{\overline{u}}$$
 (12)

With this assumption we can write the approximation to equation (9) in the interval as

$$\underline{\mathbf{M}} \ \underline{\mathbf{a}} + \underline{\mathbf{P}} (\underline{\underline{\mathbf{a}}}_{n} + \underline{\underline{\mathbf{u}}}_{n} \boldsymbol{\theta}_{1} \Delta t + \underline{\mathbf{a}} \boldsymbol{\theta}_{2} \Delta t^{2} / 2) - \underline{\mathbf{Q}} \cdot (\underline{\underline{\mathbf{p}}}_{n} + \underline{\mathbf{p}} \boldsymbol{\theta}_{1} \Delta t) - \underline{\mathbf{f}}_{1} = \underline{\mathbf{Q}} (13a)$$

$$\underline{\mathbf{u}}_{1}, (\underline{\hat{\mathbf{p}}}_{n} + \underline{\beta} \underline{\hat{\mathbf{e}}}_{1} \Delta \mathbf{t}) + \underline{\mathbf{S}} \underline{\beta} + \underline{\mathbf{q}}^{T}, (\underline{\underline{\hat{\mathbf{u}}}}_{n} + \underline{\alpha} \underline{\hat{\mathbf{e}}}_{1} \Delta \mathbf{t}) - \underline{\hat{\mathbf{f}}}_{2} = \underline{\mathbf{0}}$$
 (13b)

In above  $\theta_1$ ,  $\theta_2$ ,  $\overline{\theta}_1$  are simply parameters defined by the weighting functions

(e.g. 
$$\theta_1 = (\int_0^{\Delta t} W\tau \ d\tau) / (\Delta t \int_0^{\Delta t} W \ d\tau) \text{ etc.})$$

These parameters can take any values in the range of [0,1]. Totally implicit and unconditionally stable algorithms are available with\*

$$\frac{\theta_2 \ge \theta_1 \ge 1/2}{\tilde{\theta}_1 \ge 1/2} \tag{14}$$

In general, system of equations implied by equation (13) is in the form

$$\underline{\Psi}(\underline{\alpha},\underline{\beta}) = \underline{\Psi}(\underline{\gamma}) = \underline{0}$$
 with  $\underline{\gamma} = (\underline{\alpha},\underline{\beta})^T$  (15)

This can be solved in a variety of (iterative) ways writing

$$\chi^{i+1} = \chi^{i} - \underline{A}^{*-1} \stackrel{\oplus i}{=}$$
 (16)

where  $\underline{A}^*$  is a suitable gradient matrix approximating to

$$A^* = \partial ? / \partial \chi \tag{1.7}$$

In detail the matrix  $\underline{\underline{A}}^{\bullet}$  can be written for a Newton Raphson process as

$$\underline{\Lambda}^{\bullet} = \begin{bmatrix} \underline{M} + \underline{K} \Theta_2 \Delta t^2 / 2 & -\underline{Q} \Theta_1 \Delta t \\ -\underline{Q}^T \Theta_1 \Delta t & -\underline{I} \underline{I} \Theta_1 \Delta t - \underline{S} \end{bmatrix}$$
(18)

with  $\theta_1 = \bar{\theta}_1$  and symmetric  $\underline{M}$ ,  $\underline{K}$ ,  $\underline{H}$  and  $\underline{S}$  matrices the total system is symmetric.

In above  $\overline{\underline{K}}$  is the well known tangent stiffness matrix which for some material models currently used in soil mechanics is nonsymmetric (e.g. for nonassociated plasticity). For such materials it is convenient to use approximate expression for  $\underline{\underline{A}}^*$  for instance symmetric updates of  $\underline{\underline{A}}^{*'-1}$  using secant approximation of the BFGS type 12.

It should be remarked that assumption of incompressible behaviour ( $\underline{S}$ =0) frequently made in soil mechanics introduces no difficulty in solution of the general transient system.

THE SOIL MODEL

Using the theory of Generalized Plasticity, the following set of parameters is only required to determine the material behaviour completely.

i) <u>n</u> (loading vector)

ii) a. not (loading strain vector)

b.  $\underline{n}_{gU}$  (unloading strain vector)

iii) a. H. (loading plastic modulus)

b. H<sub>H</sub> (unloading plastic modulus)

for  $\underline{\mathbf{n}}^{\mathrm{T}} \mathrm{d}\underline{\sigma}_{e}$  > 0 the loading condition applies

and 
$$\underline{\underline{p}}_L^{-1} = \underline{\underline{p}}_e^{-1} + \frac{1}{\underline{H}_L} \underline{\underline{n}}_{gL} \underline{\underline{n}}^T$$

as for  $\underline{n}^T d\underline{\sigma}_e = 0$  then then neutral loading condition is applicable and  $\underline{D}_N = \underline{D}_e$ 

for  $\underline{n}^T d\underline{\sigma}_e$  (0 the unloading set of parameters should be used.

with 
$$\underline{D}_{U}^{-1} = \underline{D}_{e}^{-1} + \frac{1}{H_{U}} \underline{n}_{gU} \underline{n}^{T}$$

where  $d\underline{\sigma}_e = \underline{D}_e d\underline{\varepsilon}$ 

In the present study, the Pastor-Zienkiewicz Mark-3 model\* is used. For the benefit of the readers who may not be familiar with the model, a brief description of the model is included:

If crushing of the sand grains is neglected, particle re-arrangement under shear produces volumetric and shear strains related by the so-called 'dilatancy rules'.

From the experimental results obtained by Frossard<sup>13</sup> in drained triaxial tests on loading of sand, three assumptions can be made:

 Elastic strains are neglectable compared to plastic strains, and

$$d_{g} = d\epsilon_{v}^{p} / d\epsilon_{s}^{p} \simeq d\epsilon_{v} / d\epsilon_{s}$$
 (19)

where d is refered to as 'dilatancy'.

- 2. Dilatancy is independent of increment of stress or its direction for a fixed stress point.
- Dilatancy can be approximated by a linear function of stress ratio<sup>15</sup>

$$d_{g} = (1 + \alpha_{g}) (1 - \alpha_{g}) , \eta = q/p'$$
 (20)

Use of this dilatancy law has been proposed earlier by Nova and Wood<sup>14</sup>.

This simple rule predicts zero dilatancy whenever the line

$$\eta = Mg \tag{21}$$

is reached.

Generalization to three-dimensional stress conditions can be done if a law of a Mohr-Coulomb type is assumed 15 for the zero dilatancy line, giving

$$Mg = 6 \sin \phi_g' / (3 - \sin \phi_g' \sin 3\theta)$$
 (22)

where 0 is Lode's angle, defined by

$$-\pi/6 < \theta = (\sin^{-1}((3)^{3/2} J_3' / 2J_2'^{3/2}))/3 < \pi/6$$
 (23)

and

$$I'_{1} = \sigma'_{ij}\delta_{ij}/3$$
  $J'_{2} = s_{ij}s_{ji}/2$   $J'_{3} = s_{ij}s_{jk}s_{ki}/3$  (24)

 $s_{ij} = \sigma'_{ij} - \delta_{ij}I'_1$   $\theta'_g = a$  constant residual angle of friction

This zero-dilatancy rule has often been refered to as the 'critical state line', 'characteristic state line'16 or 'line

of phase transformation', a term coined by Ishihara and co-workers17.

It is to be remarked that residual failure conditions should always lie on this asymmetrical cone in the principal stress space, as rate of plastic volumetric strain has to be zero (otherwise during large continuous stress the material will either explode or collapse). Characteristic state surface is thus defined by

$$(3J_2')^{12} = -Mg I_1'$$
 (25)

The unit vector defining the direction of plastic flow is given by

$$\underline{\mathbf{n}}_{g} = (\mathbf{n}_{gv}, \mathbf{n}_{gs}) \qquad \mathbf{n}_{gv} = \frac{d_{g}}{(1 + d_{g}^{2})^{\frac{1}{2}}} \qquad \mathbf{n}_{gs} = 1 / (1 + d_{g}^{2})^{\frac{1}{2}}$$
(26)

with  $n_{\Theta\Theta}$  is defined as the appropriate outward normal in the  $\Theta$  direction with proper scaling. The direction discriminating between loading and unloading is characterized in a similiar manner:

$$\underline{n} = (n_v, n_s)$$
  $u_v = d_f/(1 + d_f^2)^{12}$   $n_s = 1/(1 + d_f^2)^{12}$  (27)

$$d_{\mathbf{f}} = (1 + a_{\mathbf{f}}) (M_{\mathbf{f}} - \eta)$$

where Mf is taken as:

$$Mf = Mfo Mg / Mgo$$
 (28)

where Mfo. Mgo are the values in the triaxial compression state. Choice of different  $\underline{n}_f$  and  $\underline{n}_g$ , i.e., non-associativeness of flow rule is introduced as a natural way of modelling unstable behaviour within hardening region.

The last term requiring definition of the loading process is the plastic modulus, for which the following expression is proposed.

$$H_L = H_0 p' (1 - \eta/\eta_f)^4 (H_V + H_s)$$
 (29)

where

$$\eta_{f} = (1 + 1/\alpha_{f}) M_{f}$$
He = 0 0 000 (30)

Hs =  $\beta_0$   $\beta_1$  exp $(-\beta_0$   $\xi)$   $\xi = \int |d\xi|$ 

d is calculated by appropriate transformation 2.3 Ho,  $\beta$ o and  $\beta_1$  being additional model parameters introduced.

η<sub>f</sub> defines a non-symmetric cone in the space of stress invariants at which plastic modulus is zero. This surface acts as a limiting one in the sense that no exterior state is possible.

Mg defines, as already explained, another non-symmetric cone characterizing those states at which shear straining takes place with no change in volumes. Residual condition take place at this surface: as for large strains, ils vanishes, giving here

$$H = H_0 P_R^* (1 - M_g/\eta_f) Hv = 0$$
 (31)

Finally, Hs characterizes material degradation under accumulated shear strain, effectively vanished as a certain 'length' of deviatoric strain path & is reached.

Unloading plasticity is introduced by defining an unloading plastic modulus Bu, and a flow direction, assumed to be given by

$$n_{gu,v} = |n_{gv}|$$
  $n_{gu,s} = -n_{gs}$   $n_{gu,\theta} = -n_{g\theta}$  (32)

where  $n_{gv}^{},\ n_{gs}^{}$  and  $n_{g\theta}^{}$  are the flow directions for loading.

Unloading modulus is taken as

$$Hu = Huo \left(\eta_{ij} / Mg\right)^{-\gamma u} \tag{33}$$

where  $\eta_{\rm L}$  is the stress ratio from which unloading takes place. Huo and  $\gamma_{\rm U}$  being appropriate constants. This law follows the experimental fact that on unloading plastic effects are more pronounced when the process initiates from high stress ratios  $^{17-22}$ .

Further effects of stress-strain history memory can be incorporated in the model with the largest intensity events fading preceding ones. This effect can be introduced by means of a new discrete memory factor multiplying the plastic modulus

$$H_{DM} = (\eta / \eta_{RFV})^{-\gamma}$$
 (34)

where  $\eta_{REV}$  is the largest value of stress ratio reached before reversal. During virgin loading of material,  $\Pi_{DM}$ , is taken as unity, but after unloading, reloading takes place with a higher plastic modulus.

### NUMERICAL RESULTS

Both the u-p formulation and the Pastor-Zienkiewicz Mark-3 model have been implemented on a research computer program in the Institute. Its prediction is checked against contribuge experiments done in Cambridge University. The parameters

for the soil model is found from the triaxial test done with the same sand used in the centrifuge experiment. The triaxial comparisons are given in Figure 1. The parameters defined are given in Table 1. These test datas are incomplete and some parameters had to be assumed from other tests of which full model comparison has been presented.

In this example, a full scale run has been performed. The experimental set up of the centrifuge is shown in Figure 2 and the corresponding Finite Element Mesh in Figure 3. The bilinear shape function is used for both solid and fluid phase. The other material parameters as extracted from the centrifuge data is shown in Table 2 together with the time-stepping data of the Finite Element analysis.

The vertical deflection of the crest of the dyke is shown in Figure 4. The result compares excellently with the experiment. The shape, the final values and the initial major increase matches the experiment perfectly. The readers are reminded that the result is obtained on the first run without any parameter adjustment. The excellent results in settlement is of great importance in practical application. The extent of total settlement is of most concern in earthquake analysis if total failure has not occurred. Also shown in Figure 4 is the input motion of the earthquake as defined as the base motion of the centrifuge experimental compartment.

Comparisons with ten pore pressure transducers have been Due to the limitation of space, only two are shown. They correspond to point A and D in Figure 3. They show a typical behaviour of the ten comparisons. The rising time and the magnitude compare well with the experiment. However, some cases, the oscillations of the results are excessive, The magnitude has been improved by a slight adjustment in the soil parameters and the oscillation is reduced if a further damping is used in the run. The result of the accelerometer at point L is shown in Figure 5. The initial cycles shown good agreement, however, the experiment shows less shear wave transmission to the top layer than the numerical prediction. But in general the results are very good. Further comparisons using other elements and other centrifuge tests are in progress.

#### CONCLUSIONS

From the comparisons of the numerical prediction and the experimental results, one can conclude that behaviour of the soil and pore-fluid under earthquake loading is essentially a two-phase phenomena and fully coupled analysis should be employed. The results show that with a properly engineered model, the numerical solution is capable to predict both settlement and pore water pressure rise to an acceptable